Tartaruga, I., Cooper, J. E., Lowenberg, M. H., Sartor, P., & Lemmens, Y. (2018). Uncertainty and sensitivity analysis of bifurcation loci characterizing nonlinear landing-gear dynamics. *Journal of Aircraft*, *55*(1), 162-172. https://doi.org/10.2514/1.C034252

Uncertainty and Sensitivity Analysis of Bifurcation Loci Characterizing Nonlinear Landing Gear Dynamics

I. Tartaruga [a] and J. E. Cooper [b], M. H. Lowenberg [c] and P. Sartor [d]
University of Bristol, Department of Aerospace Engineering,

Queens Building, University Walk, Bristol, United Kingdom, BS8 1TR

Y. Lemmens [e]
Siemens PLM Software, Aerospace Competence Center, Leuven, Belgium

A methodology is developed to efficiently, yet accurately, determine the uncertainty bounds of the bifurcation loci of nonlinear dynamic systems subjected to parametric variations. The chosen approach make use of numerical continuation, the higher order singular value decomposition and surrogate modelling. The technique is demonstrated on a representative model of an aircraft undercarriage where the effect of uncertainty in the structural parameters is propagated onto the prediction of the conditions for the onset of shimmy. Comparison with numerical integration results demonstrates the accuracy of the methodology.

[a] Marie Curie early stage PhD researcher, ALPES Project, University of Bristol, irene.tartaruga@bristol.ac.uk .
[b] RAEng Airbus Sir George White Professor of Aerospace Engineering, Dept of Aerospace Engineering, University of Bristol, J.E.Cooper@bristol.ac.uk.
[c] Professor of Flight Dynamics, Dept of Aerospace Engineering, University of Bristol, M.Lowenberg@bristol.ac.uk.
[d] Lecturer in Aerospace Engineering, Dept of Aerospace Engineering, University of Bristol, pia.sartor@bristol.ac.uk.
[e] Sr Project Leader RTD, Siemens PLM Software, yves.lemmens@siemens.com.

Nomenclature

A, U, V, $\mathbf{\Sigma}$ = matrices used in the singular value decomposition

$\mathcal{A}$, $\mathcal{S}$ = tensors adopted in the high singular value decomposition

B = number of intervals into which the locus of bifurcation points is divided

$c_\psi, c_\delta, c_\beta$ = damping coefficient of ψ, δ and $beta$ DoF

$E_{\mathbf{X}}$ = mean of the objective function f due to a change in the defined set of factors $\mathbf{X}$

f = objective function adopted in the sensitivity analysis

F_z = vertical force acting on the landing gear

$I_\psi, I_\delta, I_\beta$ = inertia of ψ, δ and $beta$ DoF

$k_\psi, k_\delta, k_\beta$ = stiffness coefficient of ψ, δ and $beta$ DoF

$\mathbf{u}_\lambda$ = unit vector

L, k_t, h = tyre relaxation length and vertical stiffness, length of contact region and

$M_\psi, M_\delta, M_\beta$ = moments acting on the the landing gear with respect to the three dynamics ψ, δ, β

n = number of factors considered in the sensitivity analysis

N = dimension of the adopted sampling plane

p = angle used to orient the landing gear

$\mathbf{q}$ = generalized coordinates

rL, rR = radius of the left and right wheel

$\mathbf{U^i}$ = unfolding matrix adopted in the high order singular value decomposition

$\mathbf{u}_\lambda$ = unit vector along the wheel axle projected on the first two dimensions

$V, \mathbf{V_{LCF}}, \mathbf{V_{RCF}}$ = forward velocity for the landing gear system and lateral velocity of left and right wheels

$V(Y), V_{\mathbf{X}}$ = total variance of the objective function $f(\mathbf{X})$ and variance due to a change in the defined set $\mathbf{X}$

X_i = factors considered in the sensitivity analysis

$\mathbf{X}_i$ = set of factors X for which just the value of X_i is changed

$\mathbf{X}_{\sim i}$ = set of factors X for which all the values are changed but the one for X_i

Y = output of the evaluated objective function f

β = DoF describing the rotation on the landing gear about the two attachment points

δ = DoF expressing the bending of the landing gear's oleo piston in the side-stay plane

λ = state of the lateral slip (meters) for the tyre model

λ_i = singular values

μ = sidestay plane

I. Introduction

The certification of real industrial sized systems requires the accurate prediction of the dynamic behaviour throughout the entire design operation envelope. As structures are being made more efficient, for instance through weight reduction or modern manufacturing techniques that reduce the number of separate components, the effects of nonlinear behaviour are becoming increasingly important. Consequently, there is a need to develop methods that can predict accurately the nonlinear dynamical behaviour and assess the effect of variations in the design and uncertainty in the operating parameters. In the aerospace field there is particular interest in the nonlinear phenomena of Limit Cycle Oscillations (LCOs) and Shimmy [1–5].

The prediction of nonlinear dynamic behaviour using full size numerical models can be extremely time consuming and, as the characteristics are initial condition dependent, requires simulated testing considering all possible states which is computationally prohibitive. Applying the same brute force approach for the characterisation of the effects of system parameter uncertainty on the response increases the computational requirement by many orders of magnitude. There are several ways that analyses can be made more feasible, including the generation of reduced order models which retain the main characteristics of interest; however, investigation of the nonlinear behaviour would still require a substantial amount of blind testing.

An alternative is to employ continuation and bifurcation analyses, which are powerful means to investigate the system stability, and to study the occurrence of multiple paths in the possible equilibrium solutions. Bifurcation is a phenomenon that is common in several dynamical systems and can be described as a sudden qualitative change in the system behaviour due to small variations in system parameters. Here we focus on Limit Cycle Oscillations (LCOs), a particular effect that can occur only in non-linear systems, which are isolated closed trajectories characterized by periodical solutions for the states of the systems, i.e. the response of the system results to be bounded and periodical. LCOs can be stable, half-stable or unstable and arise following the occurrence of a so-called Hopf bifurcation. Hopf bifurcations can occur in systems with at least two states and occur when the real part of a pair of complex eigenvalues of the Jacobian matrix of the linearised system changes sign following some system parameter variation.

There are several techniques that can be used to perform bifurcation analysis [6, 7] over the entire design envelope rather than resorting to a Monte Carlo random search, resulting in a considerable saving in computational time. Branch and bounds methods, numerical and experimental continuation approaches find a numerical and experimental solution respectively [8], whilst non-linear normal forms can be selected if an analytic solution is sought [9]. All these methods can be adopted to identify equilibrium branches of the bifurcation diagrams (including steady-state bifurcation points, such as pitchfork and saddle-node bifurcations, and Hopf bifurcations). However, not all of them solve periodical solutions (e.g. Limit Cycle Oscillation (LCO)): continuation, experimental and, ideally, pure Monte Carlo random search and non-linear normal forms can be exploited. In the case of periodical solutions, Harmonic Balance methods have also been adopted for the identification of LCOs in the aereolastic and aerodynamics fields [1–3, 10–13]. In the present paper continuation analysis is used.

A further important consideration is the uncertainty that is always present in real-life structures resulting, for example, from variations in the materials, manufacturing processes and operating conditions. Such deviations can cause significant changes in the behaviour of a wide range of systems and there is currently much interest in finding efficient ways of quantifying the effects of uncertainty [14] [15]. The traditional approach to deal with these variations is to model the system behaviour in a deterministic manner assuming no errors in the model, as seen in Fig. 1, and to then add a safety margin. Such a simple methodology tends to produce overdesigned structures. With the requirement to manufacture more efficient (e.g. lighter) structures it is apparent that non-deterministic approaches need to be used which consider both aleatory and epistemic forms [15] of uncertainty. Both stochastic and/or interval approaches can be applied depending on the uncertainties present. In real systems typically both kinds of uncertainties exist, so it is desirable to develop approaches that combine stochastic and interval methodologies in a computationally efficient manner. A further benefit of applying Uncertainty Quantification (UQ) analysis is that it is possible to determine which are the parameters whose changes have the greatest effect on the system behaviour, and also to enable robust design optimisation to be performed.

In the last decade, researchers have started to look at the effect of parametric uncertainty (structural

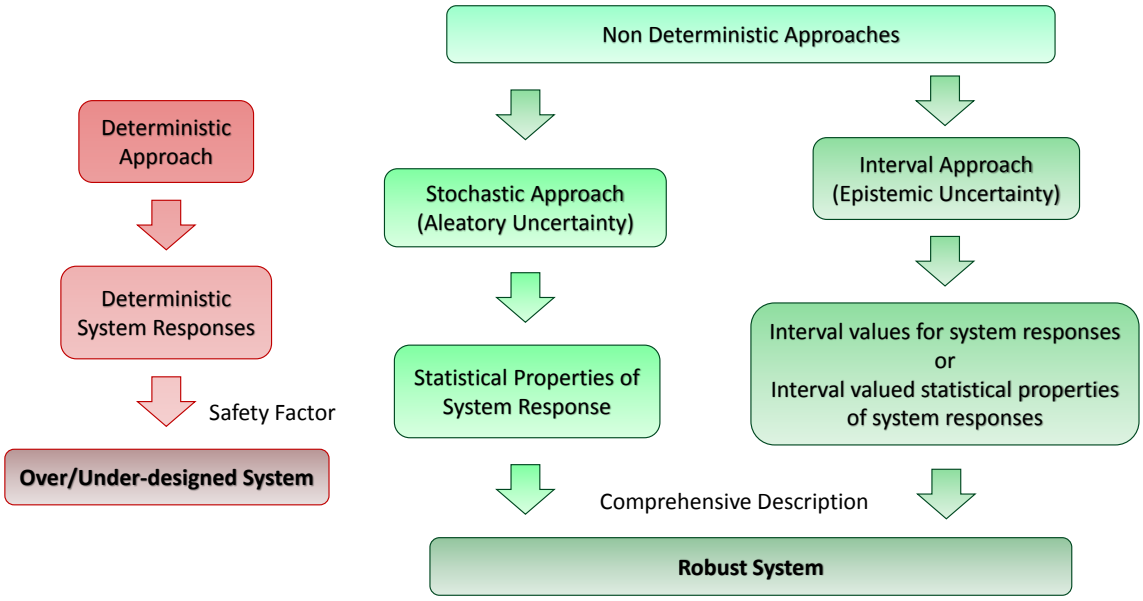

Fig. 1 Approaches in a design process.

and aerodynamic) for conventional and composite aircraft structures on the occurrence of flutter, and also the amplitude and frequency of LCOs for nonlinear aeroelastic systems [3, 14, 16–20]. For these studies, expensive time simulation studies have primarily been used and there is a need to use more efficient UQ methods.

The aim of this paper is to present a new methodology to efficiently perform the uncertainty quantification and sensitivity analysis of the bifurcation diagrams characterizing the behavior of a multi-dimensional nonlinear system. Confidence bounds are defined for the possible occurrence of LCOs in the presence of parametric uncertainty. These bounds are the loci of the Hopf bifurcation points and determine subdivision of the parameter space of interest. The methodology is implemented in Matlab, through the development of a tool that exploits the Dynamical System Toolbox [21], a Matlab interface with AUTO, the software used to perform numerical continuation analyses [22]. The uncertainty propagation has been performed through the development of an improved version of a SVD-based method adopting geometrical considerations which has already been used to predict the gust lengths that cause critical correlated aircraft loads in presence of parametric uncertainty [23–25]. The effect of parameter uncertainty is determined through the construction of surrogate

models upon which the sensitivity analysis and uncertainty quantification can be applied.
The novel methodology is demonstrated by considering a representative landing gear model and examining the effect of uncertainty in a range of structural parameters on the occurrence of 'shimmy'. It is shown how it is possible to efficiently define the operating ranges within which shimmy may occur. The approach is validated through comparison with extensive numerical simulations.

II. Case study and bifurcation analysis

The case study presented in this paper to demonstrate the developed methodology relates to the occurrence of limit cycle oscillations in a representative nonlinear aircraft landing gear system. Uncertainty quantification and sensitivity analyses are applied to the locus of the bifurcation plots, characterizing the mechanism for the loss of stability of equilibria.

A. Landing gear model

The analytic landing gear model is the one presented by Howcroft [26] representing a dual-wheel main landing gear. The ground/tire interface is the source of nonlinearities that characterize the forces generated at such an interface. These forces are included in the considered model, however the free-play and wheel gyroscopic effects are omitted. The deflection of the landing gear structure is modeled in terms of three degrees of freedom (Fig. 2) and an additional DoF is introduced for the tyre dynamics. There are seven states, since the equations for the first three DoFs are of second order while the last is of first order. The degrees of freedom are:

1. torsional, ψ, describing the rotation of the wheel/axle assembly about the local axis z;

2. in-plane, δ, expressing the bending of the oleo piston in the side-stay plane. This DoF is approximated as a rotation about a point at a distance L_δ from the axle;

3. out-of-plane, β, describing the rotation of the landing gear about the two attachment points;

4. lateral tyre displacement, λ, which is represented adopting the straight tangent model [27].

Since the sidestay plane μ has been fixed to zero, the words longitudinal and lateral are adopted to refer to the out-of-plane and in-plane DoF of the landing gear. The differential equations describing

the dynamic evolution of these states are:

Dynamics of Torsional DoF

$$I_\psi \ddot{\psi} + c_\psi \left(\dot{\psi} + \dot{\beta}\sin p\right) + k_\psi \left(\psi + \beta \sin p\right) = M_\psi \left(, \dot{q}\right) \tag{1}$$

Dynamics of Lateral DoF

$$I_\delta \ddot{\delta} + c_\delta \dot{\delta} + k_\delta \delta = M_\delta \left(q, \dot{q}\right) \tag{2}$$

Dynamics of Longitudinal DoF

$$I_{\beta_0} \ddot{\beta} \cos^2 p + \left[c_\beta \dot{\beta} + c_\psi \left(\dot{\psi} + \dot{\beta}\sin p\right) \sin p\right] + \left[k_\beta \beta + k_\psi \left(\psi + \beta \sin p\right) \sin p\right] = M_\beta \left(q, \dot{q}\right) \tag{3}$$

Tyre Model

$$\dot{\lambda} + \frac{V}{L}\lambda + \frac{1}{2}\left(V_{LCF} + V_{RCF}\right) \cdot u_\lambda = 0 \tag{4}$$

Further information on this model and the considered assumptions are provided in [26]; the nominal values of the parameters of this model are given in appendix VI.

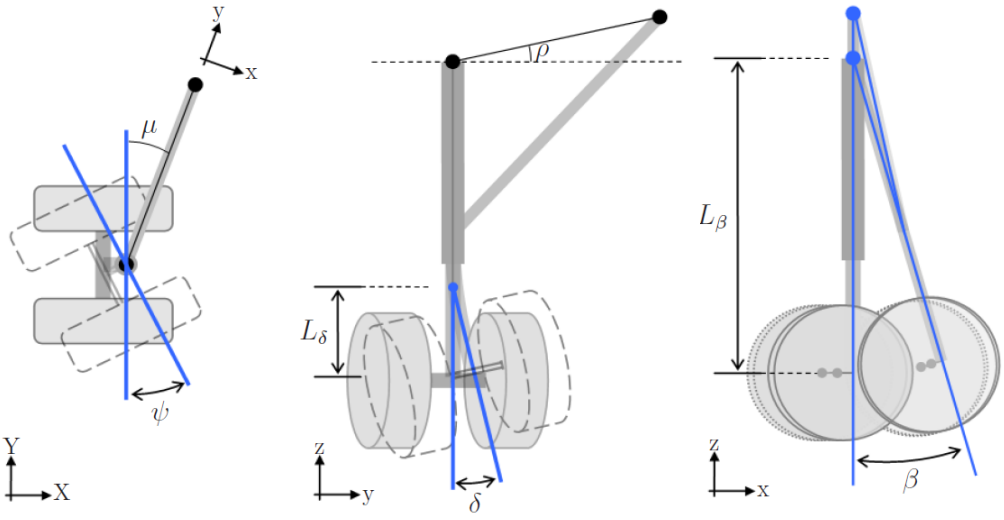

Fig. 2 Torsional ψ, lateral δ and longitudinal β degrees of freedoms. (XYZ) and (xyz) are the global and local coordinate systems.

B. Bifurcation Analysis

The implementation of bifurcation analysis entails the solution of all the steady states of the system in the parameter range of interest, along with a determination of their stability. Changes in local stability as a parameter varies are then assessed using bifurcation theory to infer the mechanisms governing the global behavior.

The results obtained from the bifurcation analyses can be graphically visualized and the plots are called bifurcation diagrams. On such diagrams the steady state behavior can be traced against design variables together with maximum amplitude of self-oscillations, if they occur, as well as the combinations of design variable values at which the system has a qualitative or topological change in its behavior.

Adopting numerical continuation, which is the technique considered here, it is first necessary to define the set of parameters to be varied in order to investigate possible changes in stability of equilibrium solutions; these parameters are called bifurcation parameters. Then equilibrium solutions need to be determined in terms of the variation of one of the selected bifurcation parameters, detecting the occurrence of possible bifurcation points such as Hopf bifurcations. In the presence of such critical points, the locus of bifurcation points can be investigated as more than one parameter changes, and shown directly on two parameter bifurcation diagrams instead of considering several one parameter bifurcation diagrams varying from one to the other the value of the second considered bifurcation parameter. Moreover, if the bifurcation point is a Hopf bifurcation, then limit cycle oscillations occur and the maximum amplitude and period characterizing the relative periodic response of the system can be determined. In addition to the bifurcation parameters, the variation of other parameters can be considered.

Having considered the *shimmy* in the landing gear as the case study, the selected bifurcation parameters are the forward velocity V and the vertical force F_z along the main structure of the landing gear, as these parameters experience a considerable variation during take-off and landing.

- The variation of the vertical force F_z is strictly related to the loading condition (for instance lift relative to weight during take-off, landing or taxing). In the present paper, an upper force limit of $4 \cdot 10^5$ N is considered.

- The forward velocity V during a landing manoeuvre must be in agreement with the certification; tables provided in an International Civil Aviation Organization (ICAO) document [28] indicate the specified range of handling speeds for each category of aircraft to perform the manoeuvres specified. These speed ranges are assumed for use in calculating airspace and obstacle clearance requirements for each procedure. Taking into account the information provided by ICAO, a range of interest $0-100$ m/s for the forward velocity V has been considered in the analysis.

Moreover, the aim of the analysis is to investigate the variation of occurrence of Hopf bifurcation points in the operational parameter space usually considered for ground manouevres, i.e. in the (F_z, V) space. Having defined F_z and V as bifurcation parameters, the variation of the locus of Hopf bifurcation points in the defined operational parameter space can be investigated as other parameters change. Figure 3 shows deterministic bifurcation diagrams in terms of one bifurcation parameter and maximum amplitude for the periodic solution; Figure 4 shows a locus of hopf bifurcation points, including both Hopf points in figure 3, in the two-parameter bifurcation diagram. The analysis has been performed using AUTO as the continuation and bifurcation software [22]. In order to clarify the possibility of considering changes in other parameters, Figures 3 and 4 present bifurcation diagrams in one (the forward velocity V) and two parameters (the forward velocity V and the vertical force F_z) for both a set of nominal values for all the parameters characterizing the landing gear model, and also a set of values in which three structural parameters (I_ψ, c_ψ, L) are changed. The velocity at which Hopf bifurcation occurs and the maximum amplitude of the periodic solutions differ for the two cases.

Looking at Figure 4, unstable equilibrium solutions characterize all the points in the convex region, i.e. above the relevant locus of Hopf bifurcation points, and here LCOs (shimmy phenomena) occur.

The methods to be considered in order to track the change of the locus of Hopf bifurcation points is presented in section III.

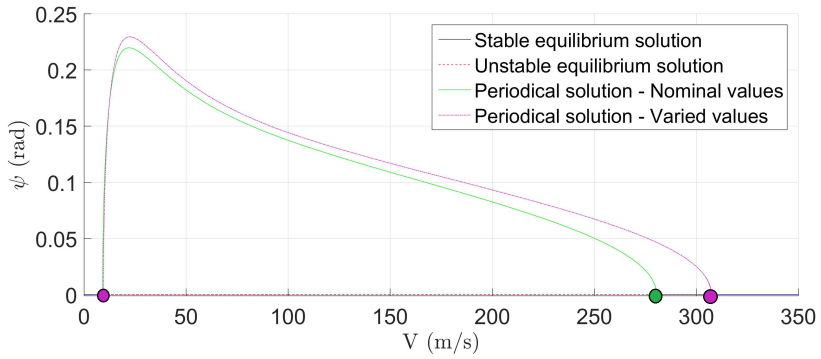

Fig. 3 Deterministic bifurcation diagrams in the forward velocity V, with periodic branches obtained for nominal and varied structural parameters values. The dot points are used to underline where the Hopf bifurcations occur and the color is related to the relative bifurcating limit cycle. The Hopf bifurcations of the two periodic branches overlapped at low velocity.

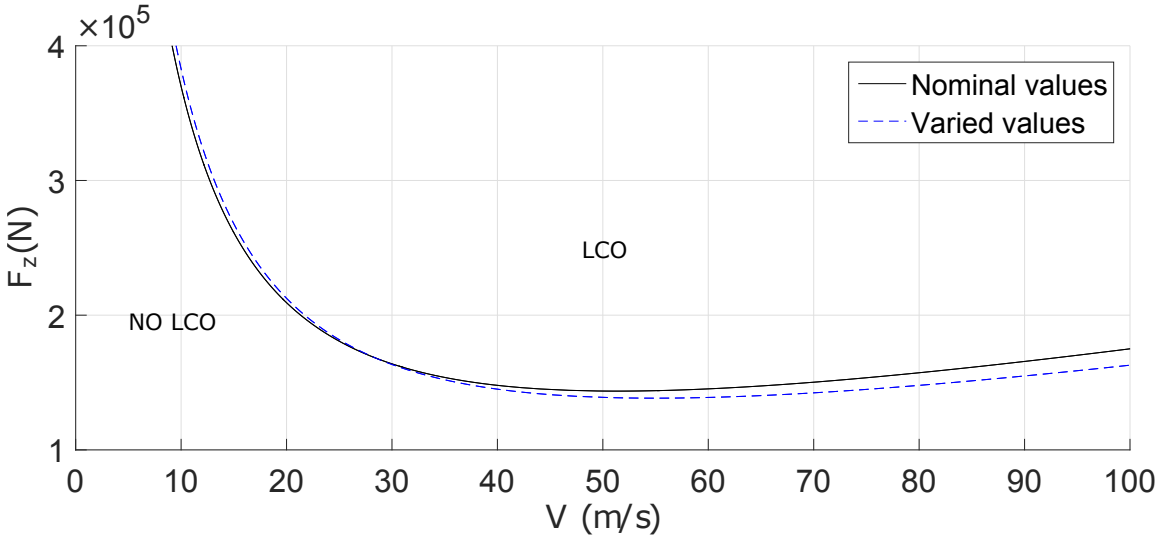

Fig. 4 Deterministic bifurcation diagrams in two parameters obtained for the design factors fixed to their nominal values and also for a case where three structural parameters are changed.

III. Methodology

Figure 5 presents the flow process chart of the methodology to define confidence bounds for the sought delimitation-branches. This approach allows the development of a suitable sampling plane for both sensitivity analysis (SA) and uncertainty quantification (UQ), running AUTO, performing bifurcation analysis, systematically evaluating the influence of parameters on the analysed landing

gear model adopting the Sobol' indices as sensitivity metrics and then performing UQ in terms of parameters 'significant' for the system.

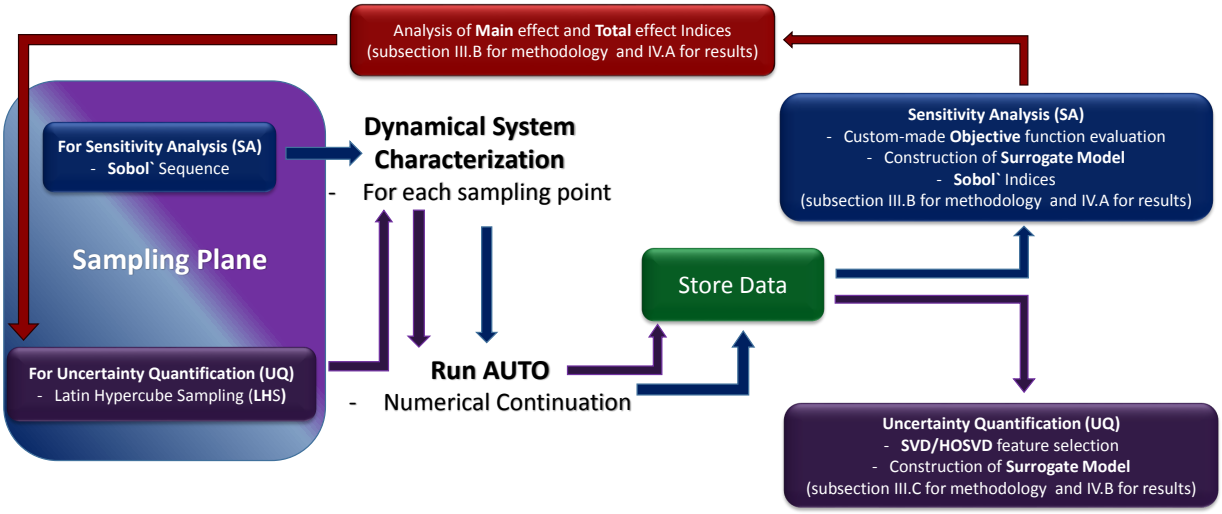

Fig. 5 Flow process chart of the tool developed to perform SA and UQ in terms of bifurcation diagrams using AUTO.

In order to perform both the sensitivity and uncertainty analysis, a suitable description of the bifurcations is needed. In the following subsections, the adopted description of the analyzed locus of points, the sensitivity metrics and the method to perform UQ are presented.

A. Description of interesting branch

The delimitation of the occurrence of LCO in the 2-parameter space (V,F_z), is described considering a fixed number of points $B+1$ for all the considered sampling points (both training and validation). These points are obtained dividing each branch into B equal intervals. In this subsection, an illustration of the description adopted for the sought branches is shown (Fig. 6). In this example B is fixed equal to 20 and each line is a 2-parameter continuation of Hopf bifurcations obtained at a particular sampling point.

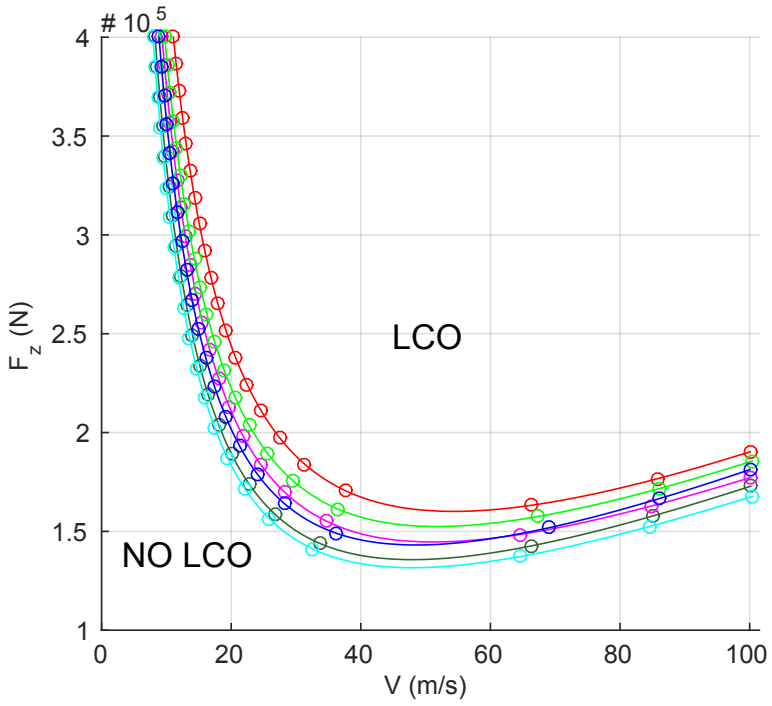

Fig. 6 Example of the description adopted for the sought branches to perform both the Sensitivity Analysis and the Uncertainty Quantification.

B. Sensitivity Analysis

SA has its origin in the design of experiments (DOE), which was introduced in order to evaluate the input/output (I/O) relation in the presence of variation in factors, which can be both parametric (such as structural features) and non parametric (such as environmental conditions). '*Sensitivity analysis* studies the relationships between information flowing in and out of the model' [29]. SA is directly correlated to and is a means to cope with the *uncertainty*. As remarked by Saltelli [29], there is not a '*universal recipe*' that explains how to conduct a SA and which measures should be adopted. The decision for the method and sensitivity measures to be adopted depends on the particular problem, model and accepted computational cost.

In the analyzed problem, the most significant parameters are sought to perform UQ in terms of the locus of Hopf bifurcation points and for this aim sensitivity metrics that capture non-linear dynamical behaviour and high order interaction are desirable. For this reason the main effect S_i and the total effect indices S_{T_i} have been selected. These are part of the *global* SA methods and are able

to correlate the variation in the objective function of interest $f(\mathbf{X})$ with the variation in n selected factors $(X_1, X_2, ..., X_n)$ exploiting statistical means and usually adopting a sampling approach. In particular, S_i measures the variation in f due to a change in just one factor X_i and the sum of all the indices $\sum_{i=1}^{n} S_i$ is less or equal to 1. S_{T_i} measures the variation in the objective functions f due to the change in all the factors rather than X_i and the sum of all the indices $\sum_{i=1}^{n} S_{T_i}$ must be greater than or equal to 1. The equality occurs only in the case of a perfect additive model and in that case $\sum_{i=1}^{n} S_i = 1$. There are as many main or total effect indices as the number n of selected factors X . Saltelli has emphasized the importance of S_{T_i} [29]-[32], which measures the total effects (i.e. first and higher order iterations) of factor X_i, especially in the presence of a very large number of factors.

The main S_i and total effects S_{T_i} are obtained as [30]

$$S_i = \frac{V_{X_i}(E_{\mathbf{X}_{\sim \mathbf{i}}}(Y|\, X_i))}{V(Y)} \tag{5}$$

$$S_{T_i} = \frac{E_{\mathbf{X}_{\sim \mathbf{i}}}(V_{X_i}(f|\, \mathbf{X}_{\sim \mathbf{i}}))}{V(Y)} = 1 - \frac{V_{\mathbf{X}_{\sim \mathbf{i}}}(E_{X_i}(Y|\, \mathbf{X}_{\sim \mathbf{i}}))}{V(Y)} \tag{6}$$

where Y is the output of the objective function of interest f, $E_X(\cdot)$ and $V_X(\cdot)$ are the mean and variance of argument $(\cdot)$ over $\mathbf{X_i}$, while $E_{\mathbf{X}_{\sim \mathbf{i}}}(\cdot)$ and $V_{\mathbf{X}_{\sim \mathbf{i}}}(\cdot)$ are the mean and variance of all factors but X_i. $\mathbf{X}_{\sim \mathbf{i}}$ and $\mathbf{X_i}$ stand for the set of factors X for which all the values are changed but the one for X_i and just the value of X_i is varied, respectively. $V(Y)$ is the total variance of the objective function $f(\mathbf{X})$.

In order to efficiently perform the SA, a computational approach that allows a simultaneous computation of S_i and S_{T_i} has been adopted and the indices are evaluated using a surrogate model (obtained via Blind Kriging [33]-[35]) developed for each selected objective function f, trained and validated with a suitable number of sampling points, adopting Sobol' sequences (also known as LP_τ sequences) as the quasi-Monte Carlo algorithms [29]. An analytical evaluation of such indices is feasible only for simple systems, which is not the case here. The considered numerical computation has been presented by Saltelli in [30] [37] to which the reader can refer for further information. Here

it is worth mentioning that there are 12 possible combinations [38] to calculate the total variance $V(Y)$. In the present analysis, all of these combinations have been considered and compared in order to find out the one that gives the most coherent result with respect to the stated properties of the indices and with the lowest computational time for convergence.

In order to consider the importance of the design parameters, and so determine the Sobol' indices, it is important to select suitable functions f, used as 'objective' functions for the Sobol' indices. For the landing gear system f has been defined having fixed the two parameters that are considered as the operating ones due to their importance for the dynamics of a landing gear system: the forward velocity V and the vertical force on the landing gear F_z. The qualitative change in the solution branches can be captured if the objective functions describe both variation in the **shape** and **translation** of the interesting branches. To this end the branches are divided into an equal number of intervals B as discussed in III A; an example of the stated division and the qualitative change aimed to be detected is shown in Fig. 7, fixing B equal to 12 and labeling with b the points used for the discretization ($b = 1, ..., B+1$). The figure shows that the starting point for the bifurcation diagrams presents the same value for the vertical force F_z; in fact the continuation in two parameters is performed starting and ending the bifurcation branches always at the same value for the vertical force F_z.

To capture the qualitative change of the locus of bifurcation points in the two parameter space identified by V and F_z, two kinds of objective functions have been selected:

1. for each determined segment on the analysed branches, the approximated slope is taken as an objective function to capture changes in the **shape** of the analysed branch

$$f_{1b_{i_1...i_s}}(X_{i_1...i_s}) = \frac{\partial F_z}{\partial V}(X_{i_1...i_s})\bigg|_b \simeq \frac{\Delta F_z}{\Delta V}(X_{i_1...i_s})\bigg|_b \qquad b = 1...B \quad 1 \leq i_1 < ... < i_s \leq N \tag{7}$$

2. at the first determined Hopf bifurcation point, i.e. at which the continuation has been switched in two parameters, the velocity $V_{b=1} = V_1$ is considered as an objective function to discuss **translations** of the interesting branch. It is worth mentioning that the variation in terms of the vertical force F_z could also be considered but this is not necessary here since the same

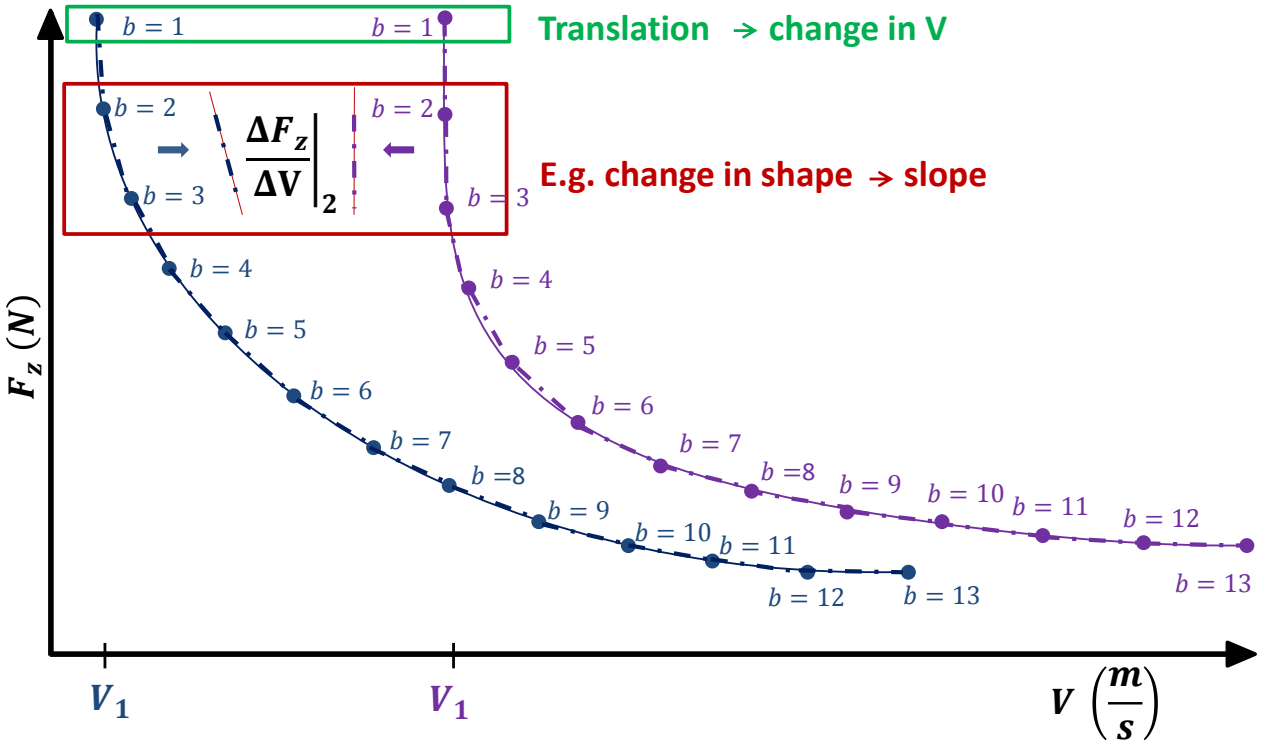

Fig. 7 Variations to be considered to capture the qualitative change in the solution branches in the parameter space of interest.

value has been adopted for all the bifurcation diagrams.

$$f_{2_{i_1 \ldots i_s}}\left(X_{i_1 \ldots i_s}\right) = V_1\left(i_1 \ldots i_s\right) \qquad 1 \leq i_1 < \ldots < i_s \leq N_P \tag{8}$$

where N_P is the number of analyzed parameters and s is the number of factors changed to evaluate the variation in the objective function. In total $B+1$ objective functions are considered. The objective functions related to the change in the shape, which are B, have to be considered as a whole since since they all describe the change in the **shape** of the solution branch of interest. Thus, for each identified branch the mean of the main and total effect indices in terms of all the B objective functions related to the shape have been considered.

If a significant topology variation of the bifurcation diagram occurs when changing a particular parameter, then this should be considered as an operating parameter. Once the SA is accomplished, then the UQ can be performed in terms of the most influential uncertain parameters. In the following subsection the adopted technique is presented. It is based upon the same principles

characterizing the already tested technique developed by the authors to predict and propagate parametric uncertainties in terms of correlated time-history quantities [23].

C. Uncertainty Quantification

The Uncertainty Quantification has been performed using a speed-up process already implemented by the authors to propagate uncertainty in terms of correlated aircraft loads [23–25]. The speed-up process has been developed using the Singular Value/High Order Singular Value Decomposition (SVD/HOSVD) and surrogate modelling technique. Then, a geometric based approach has been developed to determine the outer bounds for the occurrence of shimmy and probabilistically described occurrence of Hopf bifurcation points in the (F_z, V) parameter space.

The SVD/HOSVD is considered here for feature extraction. In particular, the terms to be retained in order to speed up the process are identified by fixing the maximum acceptable error caused by the rank reduction. Once this error is chosen, the energy 'captured' by the reduced matrix/tensor (captured energy criterion [39]) and the singular values to be retained can be identified. The stated energy is linked with the Frobenius norm and is adopted by the captured energy criterion to identify the rank reduction. The new method overcomes the difficulties in identifying the best rank reduction using the SVD/HOSVD. Indeed the energy criterion tackles the issue purely mathematically and the physics of the analyzed problem is lost. The captured energy criterion consists of selecting enough singular values of the matrix of interest, the unfolding matrix $\mathbf{A_{(1)}}$ for the considered HOSVD [25], such that the sum of their squares is a certain percentage T of the total sum of the squared values. The reason for such a decision is that the resulting matrix 'captures' $T\%$ of the Frobenius norm of the full matrix, which is correlated with the energy. In the method proposed here, the singular values characterizing the SVD or the HOSVD are automatically obtained once the stated maximum acceptable error is defined; moreover, the percentage $T\%$ can also be obtained to prove that the threshold one should consider for $T\%$ is not absolute and often difficult to be known a priori. The authors have considered an iterative procedure; the number of singular values is increased, and so the percentage $T\%$, and the rank reduction coherently updated until the desired maximum error is met. Finally, regarding the error metric, the Mean Average Percentage Error (MAPE) is considered and the average is in terms of all the considered training points.

Regarding the geometric based method, Figure 8 presents the steps that need to be followed.

1. the lower and upper bounds of the locus of Hopf bifurcation points are automatically identified thanks to geometric considerations and discretized in an equal number of points; the corresponding points are indexed with the same number.

2. directions of interest are defined as the line connecting the points with the same index and at the lower and upper bound.

3. the SVD/HOSVD based method [23–25] is then considered to determine loci of Hopf bifurcations for an arbitrary number of points in the sampling plane defined in terms of the uncertain parameters. Thus, considering the intersection of the determined locus of Hopf bifurcations with the direction of interest, a probabilistic description in terms of the locus of Hopf bifurcation points can be drawn.

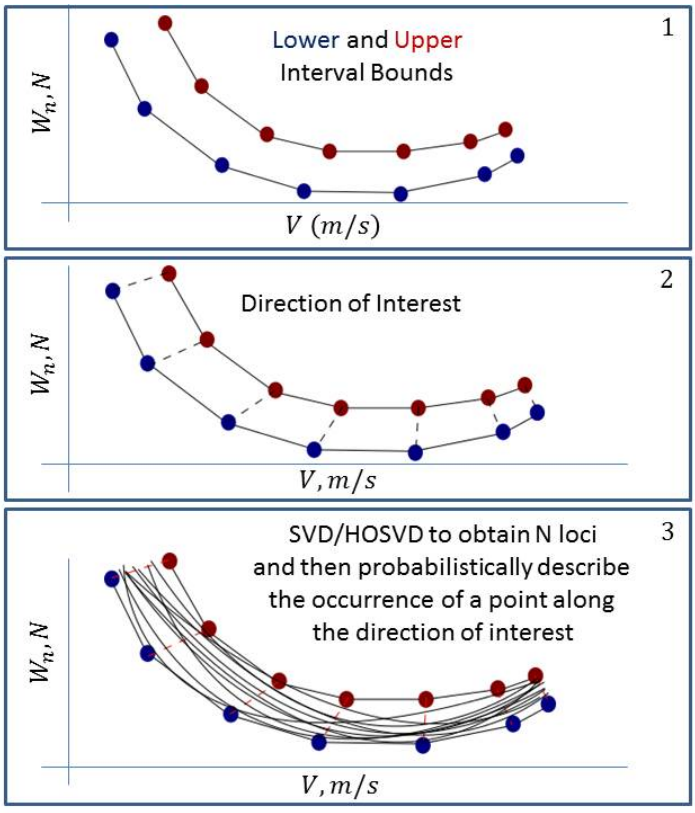

Fig. 8 Steps to be followed to apply the geometrical based method.

After having evaluated N loci of Hopf bifurcation points using the SVD/HOSVD based method,

first the worst lower and upper bounds for the locus of Hopf bifurcation points are determined and discretized in the selected $B + 1$ points. Thus, the directions of interest are identified by the pairs of points at the lower and upper bounds at the same index of discretization. Ultimately, the intersections between the N generated loci of Hopf bifurcations and each of the defined directions of interest are determined. Thus, probability density functions (PDFs) and cumulative density functions (CDFs) are defined along each direction of interest and in terms of the distance of the determined intersecting points from the points on the same direction of interest and on the lower bound. A locus of Hopf bifurcation points for a desired quantile value can be identified.

Thanks to the geometrical based method, the probabilistic description keeps information of the correlation between the selected bifurcation parameters along the direction of interest.

IV. Application and Results

The methodology developed to deal with uncertainty in complex systems are applied here to a landing gear model. First, the validation of the surrogate models adopted in the SA and the main and total effect indices are discussed. Then the validation of the surrogate models adopted in the SVD/HOSVD based method and the output given by the uncertainty propagation will be presented.

A. Sensitivity Analysis

The parameters and relative range considered to perform the SA, i.e. calculate the main and total effect indices, are shown in Table 1. Log-uniform and uniform probability distributions have been adopted if the variation of the analysed parameter is greater than or less than one order of magnitude, respectively. This choice is due to a lack of information about the parametric uncertainty [29]. For the sake of completeness, Table 1 shows which probability distribution has been adopted for each parameter.

The parameters that have not been considered in the SA are those related to:

- the longitudinal DoF β, since the side stay angle μ (also known as horizontal attachment point orientation angle) has been fixed equal to zero (as if it was a nose landing gear) and in such a configuration the longitudinal dynamics is less influential [40];

- the parameters characterizing the adopted straight tangent model for the tyre, since the whole

Table 1 Parameters and the range of values adopted in the Sensitivty Analysis

Parameter	Label	Maximum	Minimum	Units	PDF
stiffness coefficient of ψ DoF	k_ψ	963000	837000	N m rad^{-1}	log-uniform
stiffness coefficient of δ DoF	k_δ	6420000	5580000	N m rad^{-1}	log-uniform
inertia of ψ DoF	I_ψ	107	93	kg m^2	uniform
inertia of δ DoF	I_δ	428	372	kg m^2	uniform
damping coefficient of ψ DoF	c_ψ	1284	1116	N m s rad^{-1}	log-uniform
damping coefficient of δ DoF	c_δ	535	465	N m s rad^{-1}	log-uniform
radius of the left wheel	r_L	0.59	0.5487	m	uniform
radius of the right wheel [a]	r_R	0.59	0.5487	m	uniform
tyre relaxation length	L	0.5671	0.4929	m	uniform
length of contact region	h	0.2889	0.2511	m	uniform
vertical stiffness of tyres	k_t	1716280	1491720	N m^{-1}	log-uniform

[a] A different tyre tread wear level is allowed for the two wheels, represented by two separate values of their radii.

model itself is made on an assumption and so would require an uncertainty analysis on its own;

- geometrical distances that are well defined during the design process and difficult to change

during the life of an aircraft, for instance the half track width or the caster length.

In order to determine the desired main and total effect indices, the dimension N of the matrices characterizing Saltelli's technique (subsection III B) has been fixed equal to 15; thus 195 continuations in V and F_z have been computed using AUTO to identify the locus of Hopf bifurcation in the (V, F_z) parameter space. Then, fixing B, the number of discrete partial derivatives, equal to 20, the obtained data have been post-processed thus identifying the pairs (V, F_z) related to $B+1$ points of each branch. Thus, surrogate models for the selected objective functions u (slope and translation, subsection III B eq. (7) and (8)) have been constructed using Sobol' sequences as a quasi-Monte Carlo sampling plane.

The obtained surrogate models have been validated considering 10 validation points. The $MAPE$ in all the slopes for the first objective functions is always less than $3.9 \cdot 10^{-1}$ and the one in terms of the variation of the forward velocity for the second objective functions is $6.95 \cdot 10^{-2}$.

It is apparent that the trained surrogate model replicates the actual objective functions with high accuracy.

Using the surrogate models, Saltelli's technique has been adopted to evaluate the main and total effect indices. All the 12 combinations to determine the total variance V have been considered (subsection III B) and compared, adopting different numbers of evaluations of the surrogate models to test the performance in terms of convergence. Two of the considered combinations give the best convergence and are given by

$$\hat{V} = \frac{1}{N-1} \sum_{j=1}^{N} f^2(\mathbf{A}) - \hat{f}_0^2 \tag{9}$$

$$\hat{V} = \frac{1}{N-1} \sum_{j=1}^{N} f^2(\mathbf{B}) - \hat{f} \tag{10}$$

where $\hat{f}_0^2 = \frac{1}{N} \sum_{j=1}^{N} f(\mathbf{A}) f(\mathbf{B})$.

Finally, considering the first of the best two combinations (eqn. (9)), the main and total effect indices are evaluated for both the considered objective functions in order to select the parameters

to be adopted for the UQ, i.e. those most influential; both the objective functions show that I_ψ, c_ψ and L are the most influential parameters.

This is illustrated in the bar plot of the total effect indices for all the parameters (Fig. 9). For the sake of conciseness, just the mean of the adopted index related to the slope-objective functions is shown, that is

$$\overline{S}_{T_i} = \frac{1}{B}\sum_{b=1}^{B}(S_{T_i})_b \tag{11}$$

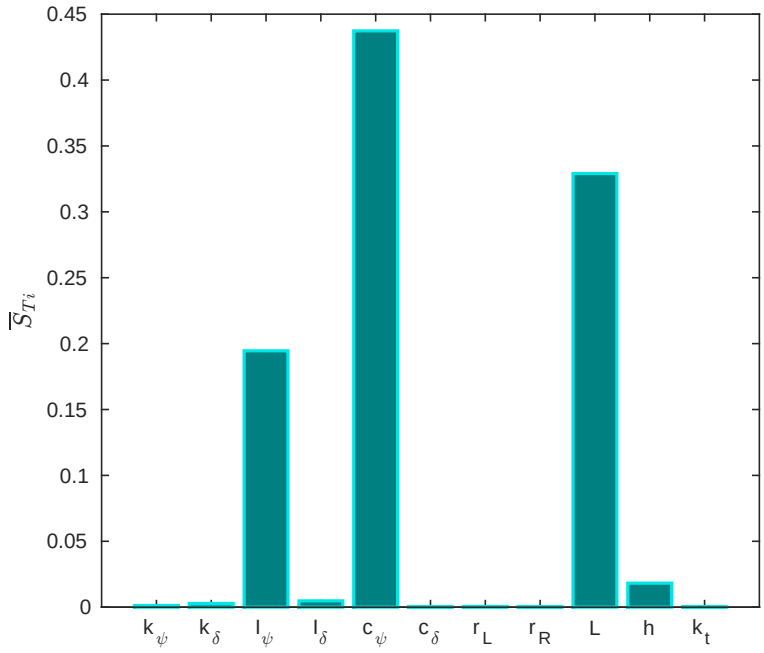

Fig. 9 Comparison of the influence of each parameter on the output considering the mean of the total effect S_{T_i} related to the slope objective function.

The obtained results are totally coherent with the *shimmy* phenomenon: *shimmy* is primarily related to the tyre characteristics and, for the analysed branch, to the torsional dynamics. In fact, looking at the LCOs generated by each of the analysed points on all the determined branches, the torsional state ψ always presents the greatest amplitude and is almost in phase with the state λ of the tyre dynamics; this means that the torsional mode is dominant in the LCOs. It can be also

noticed that the period of the LCOs is in practice always around that characterizing the linearised torsional mode: the period of the LCOs is always about $6 - 7 \cdot 10^{-2}$ sec and the damped natural period of the linearised torsional mode is $6.76 \cdot 10^{-2}$ sec.

On the basis of this SA, the validation of the surrogate models and the determined confidence bounds are provided in the following subsection.

B. Uncertainty Quantification

The performed UQ in terms of the delimitation-branches of the occurrence of LCOs has been performed in terms of the three most influential parameters, I_ψ, c_ψ and L, whose range and probability distribution have been discussed in subsection IV A and shown in Table 1.

The loci of Hopf bifurcation points are discretized using 31 points. The surrogate model adopted for the uncertainty quantification is Blind Kriging. As stated in section III C the percentage $T\%$ and the singular values (surrogate models) to be retained using the SVD and the HOSVD reduction can be determined after having fixed the maximum acceptable error due to the rank reduction. The error metric is the Mean Average Percentage Error (MAPE), whose maximum value is fixed equal to 0.1%. Tables 2 shows the percentage $T\%$ and the singular values, i.e. the rank reduction and the number of surrogate models, to be retained in order to fulfill the desired accuracy (MAPE ≤ 0.1) having considered the SVD or the HOSVD. The analysis shows that more surrogate models are required if the SVD is adopted as the reduced rank is higher. Moreover, the presented results show that the proposed method to identify the rank reduction is more valid and 'stable' than the energy captured criterion. In fact, it is apparent that a-priori such a high percentage of energy $T\%$ could not have been easily predicted as a threshold at all. The word 'stable' is used here to characterize the proposed method in the meaning that changing the data set, the technique always works well in identifying the desired rank reduction even if the corresponding energy-threshold $T\%$ changes.

	SVD F_z	SVD V	HOSVD
$T(\%)$	$100 - 10^{-6}$	$100 - 10^{-5}$	$100 - 10^{-13}$
N model	5	6	10

Table 2 Comparison of rank reduction required using the SVD and the HOSVD having fixed the maximum acceptable error.

The adopted iterative code to select the right number of singular values to be retained (and surrogate models to be trained) gives very good results. 100 and 1000 are the number of sampling points used to train and validate the adopted surrogate models respectively. The mean of the MAPE in all the discretized points in terms of the forward velocity V and the vertical load F_z is less than 1.98% and 0.26% if the SVD is considered, and less than 2.5% and 0.26% if the HOSVD is adopted.

Regarding the propagation of the uncertainties, figure 10 shows the determined lower and upper bounds adopting either the SVD or the HOSVD and these are validated using a Monte Carlo Simulation (MCS) with 1000 points. Looking at the obtained results for the uncertainty propagation it is apparent that there is just a slight lack of accuracy in terms of the forward velocity where the slope of the locus of Hopf bifurcation is almost constant. In these points the maximum $MAPE$ for V is 6% on the upper bound and 3.7% on the lower bound, for both the SVD and the $HOSVD$. Without considering such points the $MAPE$ for V and F is always less than 2%. Moreover, figure 10 shows also the direction of interest considered and two example of PDFs along such a direction. The PDFs are related to the two directions of interest the arrows are pointing at. The PDFs are first obtained in terms of the distance from the lower bound of the locus of Hopf bifurcations along the stated direction of interest, then can be projected in terms of the selected bifurcation parameters (the forward velocity V and vertical force F_z as shown in figure 10.

Adopting the probabilistic approach, one can select the lower and upper quantiles and then identify the uncertain 'tube' in which the locus of Hopf bifurcations lies. The bounds of such an uncertain 'tube' are the lines corresponding to those obtained for the selected quantiles. For the sake of simplicity, eleven values for the quantiles have been selected and presented in Figure 11, considering only the SVD based method. The HOSVD gives almost the same results. There is a lack of accuracy in the tail of the PDFs along the direction of interest for quantiles greater than 0.99. Thus the validation has been done considering quantiles less than 0.99 (Fig. 11).

The mean of the $MAPE$ for (V, F_z) determined for all the considered quantiles is less than $(0.89\%, 0.28\%)$ and $(0.87\%, 0.29\%)$ considering the SVD and HOSVD, respectively.

The performed uncertainty quantification shows similar results if the SVD or the HOSVD techniques are adopted. The HOSVD required one less surrogate models for the same fixed maximum

acceptable $MAPE$. Using the geometrical based method and the SVD/HOSVD technique, a reduction of 95% of the computational time compared to MCS is achieved whilst maintaining a good accuracy.

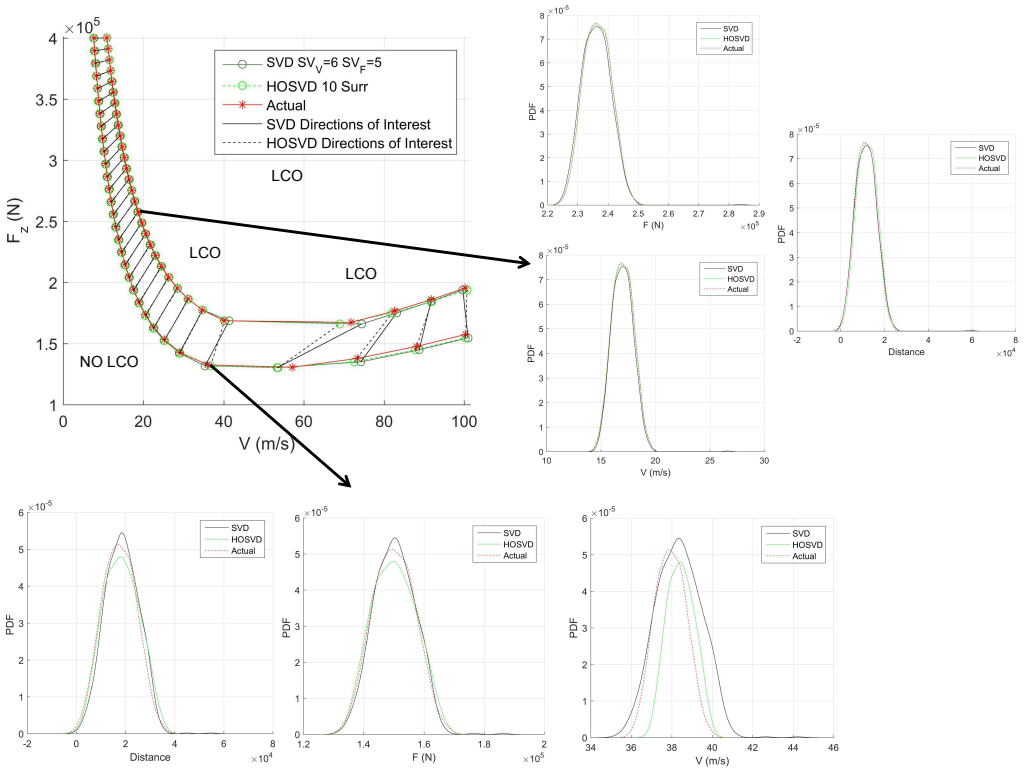

Fig. 10 Lower and upper bound for the locus of Hopf bifurcation. The results obtained using the SVD, $HOSVD$ and MCS (actual) are presented together with the adopted probabilistic description.

V. Conclusions

The paper has presented a novel approach to quantify the effect of uncertainties on multi-dimensional nonlinear systems, and in particular to identify the most influential parameters and to efficiently determine the confidence bounds of the bifurcation branches defining the regions of possible Limit Cycle Oscillations. The methodology has been demonstrated successfully on the occurrence of shimmy of a representative model of an aircraft landing gear, and comprises a Singular Value Decomposition based approach to determine surrogate models of the effect of the different system parameters on the shimmy onset speed. The proposed method to detect the number of

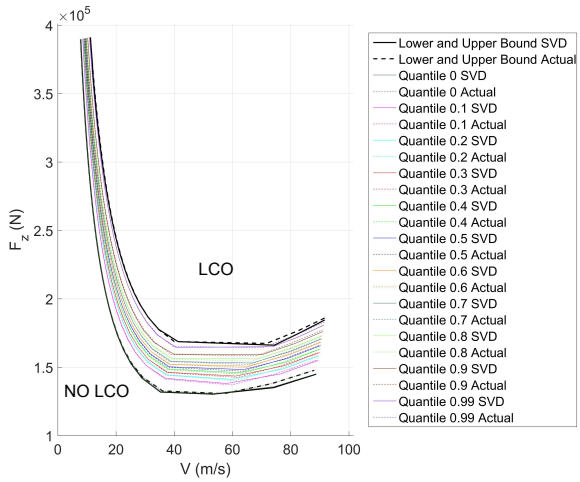

Fig. 11 Validation of the interval and quantile confidence bounds determined with the SVD based developed method. The results obtained through MCS are considered as the actual ones.

singular values to be retained is able to capture the physics behind the data set, in contrast of the mainly mathematical energy capture criterion. Comparison with Monte Carlo Simulations shows an excellent accuracy of the new approach and a reduction of almost 95% of the required computation time. Finally, it is worth remarking that the current approach dealt with system for which the topology in the analysed range of parameters doesn't change; if this occur then an extension of the developed method can be considered. A possible idea the authors have been considering is to perform a categorization of the topological behaviour and subdivide the range of variation of the parameters accordingly.

VI. Appendix

Table 3 provides the nominal values adopted for parameters characterizing the adopted dual-wheel landing gear model [26].

Acknowledgment

This work is supported by the European Commission (EC FP7) under the Marie Curie European Industrial Doctorate Training Network 'ALPES' (Aircraft Loads Prediction using Enhanced Simulation) and also the Royal Academy of Engineering. The author wishes also to thank A.

Table 3 Nominal landing gear parameters.

μ	0.0	rad/s
I_ψ	100.0	kg m^2
c_ψ	1200.0	N m s rad^{-1}
k_ψ	9.0×10^5	N m rad^{-1}
I_δ	400.0	kg m^2
c_δ	500.0	N m s rad^{-1}
k_δ	6.0×10^6	N m rad^{-1}
I_{β_0}	5000.0	kg m^2
c_β	2.0×10^4	N m s rad^{-1}
k_β	1.0×10^7	N m rad^{-1}
L	0.53	m
ρ	0.0	rad
ϕ_0	-0.1175	rad
L_β	2.818	m
L_δ	0.6	m
$r_L = r_R = r$	0.59	m
$h_L = h_R = h$	0.27	m
e	0.0	m
a	0.46	m
k_t	1.604×10^6	N m^{-1}
λ	1	m
c_λ	3000.0	N m^{2}rad^{-1}
k_λ	0.01	rad^{-1}
k_α	1.3256	m
α_m	0.1571	rad

Cammarano for the exchange of opinions.

References

[1] Dimitriadis, G., "Continuation of Higher-Order Harmonic Balance Solutions for Nonlinear Aeroelastic Systems," *Journal of Aircraft*, Vol. 45, No. 2 (2008), pp. 523-537. DOI: 10.2514/1.30472

[2] Dimitriadis, G., Vio, G. A., and Cooper, J. E., "Application of Higher-Order Harmonic Balance to Non-Linear Aeroelastic Systems," *Proceedings of the 47th AIAA/ASME/ASCE/AHS/ASC Structures, Structural Dynamics, and Materials Conference*, Newport, Rhode Island, 2006.

[3] Hayes, R., and Marques, S., "Uncertainty quantification for LCO using an Harmonic Balance method". *Proceedings of the International Forum for Aeroelasticity and Structural Dynamics (IFASD)*, 2013.

[4] Tartaruga, I., and Cooper, J. E., and Sartor, P., and Lowenberg, M. H., and Coggon, S., and Lemmens, Y., "Evaluation and Uncertainty Quantification of Bifurcation Diagram: Landing Gear, a case study". *Proceedings of the UNCECOMP 2015*, Crete Island, Greece - 25-27 May 2015.

[5] Tartaruga, I., and Lemmens, Y., and Sartor, P., and Lowenberg, M. H., and Cooper, J. E., "On the influence of longitudinal tyre slip dynamics on aircraft landing gear shimmy". *Proceedings of the ISMA2016 & USD2016 conferences*, Leuven, Belgium - 19-21 September 2016.

[6] Strogatz, S. H., *Nonlinear Dynamics And Chaos: With Applications To Physics, Biology, Chemistry, And Engineering Studies in Nonlinearity*. Westview Press, Studies in Nonlinearity, 2014.

[7] Guckenheimer, J., and Holmes, P., *Nonlinear Oscillations and Dynamical Systems and Bifurcations of Vector Fields*. Springer, Series Applied Mathematical Sciences, Vol. 42, 1983.

[8] Smith, A. P., Crespo, L. G., Muñoz, C. A., and Lowenberg, M. H., "Bifurcation Analysis Using Rigorous Branch and Bound Methods". *IEEE Multi-Conference on Systems and Control*, 2014. DOI: 10.1109/CCA.2014.6981612.

[9] Hill, T. L., Green, P. L., Cammarano, A., and Nield, S. A., "Fast Bayesian identification of multi-mode systems using backbone curves". *Journal of Aircraft*, 2008, vol. 45 n. 2. DOI:10.1016/j.jsv.2015.09.007

[10] Vio, G., and Dimitriadis, G., and Cooper, J. E., "Improved Implementation of the Harmonic Balance Method". *Proceedings of the 48th AIAA/ASME/ASCE/AHS/ASC Structures, Structural Dynamics, and Materials Conference*, Honolulu, Hawaii, Apr. 23-26, 2007.

[11] Amuyedo, N., and Cooper, J. E., "Higher Order Harmonic Balance Analysis of an Airfoil with a Hysteretic Non-Linearity". *Proceedings of 48th AIAA/ASME/ASCE/AHS/ASC Structures, Structural Dynamics, and Materials Conference*, Honolulu, Hawaii, Apr. 23-26, 2007.

[12] Amuyedo, N., and Cooper, J. E., "A Higher Order Harmonic Balance Approach for an Aeroelastic Airfoil with a Freeplay Control Surface" *Proceedings of ISMA 2008*, Leuven, Belgium.

[13] Khodaparast, H. H., and Madinei, H., and Friswell, M. I., and Adhikari, S., and Coggon, S., and Cooper, J. E., "An extended harmonic balance method based on incremental nonlinear control parameters." *Mechanical Systems and Signal Processing*, Vol. 85, p. 716-729, 3 Sep 2016. DOI: 10.1016/j.ymssp.2016.09.008

[14] Scarth, C., Sartor, P., Cooper, J. E., Weaver, P., and Silva, G. H. C., "Robust Aeroelastic Design of Composite Plate Wings". *Proceedings of 17th AIAA Non-Deterministic Approaches Conference*, Orlando, Florida USA, January 5-9, 2015.

[15] Choi, S. K., Grandhi, R. V., and Canfield, R. A., *Reliability-based Structural Design*. Springer-Verlag London Limited, 2010.

[16] Georgiou, G., Manan, A., and Cooper, J. E., "Modeling Composite Wing Aeroelastic Behaviour with Uncertain Damage Severity and Material Propertiess". *Mechanical Systems and Signal Processing*, Vol. 32, pp. 32-43, October, 2012.

[17] Badcock, K. J., Khodaparast, H. H., Timme, S., and Mottershead, J. E., "Calculating the Influence of Structural Uncertainty on Aeroelastic Limit Cycle Response". *Proceedings of 52nd AIAA/ASME/ASCE/AHS/ASC Structures, Structural Dynamics, and Materials Conference*, April 4-8, Denver, Colorado, 2011.

[18] Ouyang, Q., Chen, X., and Cooper, J. E., "Robust Aeroelastic Analysis and Optimization of Composite Wing Under Îij-Analysis Framework". *Journal of Aircraft*, Vol. 50, pp. 1299-1305, Florida USA, 2013. DOI: 10.2514/1.C031915

[19] Beran, P. S., Pettit, C. L., and Millman, D. R., "Uncertainty quantification of limit-cycle oscillations". *Journal of Computational Physics*, Vol. 217, pp. 217-247, 2006. DOI: 10.1016/j.jcp.2006.03.038

[20] Riley, M. E., Grandhi, R. V., and Kolonay, R., "Quantification of Modeling Uncertainty in Aeroelastic Design". *Proceedings of 51st AIAA/ASME/ASCE/AHS/ASC Structures, Structural Dynamics, and Material Conference*, Orlando, Florida USA, April 12-15, 2010.

[21] http://seis.bris.ac.uk/ ec1099/, date accessed November, 2015.

[22] Doedel, E., and Oldeman, B., *Auto-07p: Continuation and Bifurcation Software*, 2012. http://www.dam.brown.edu/people/sandsted/auto/auto07p.pdf downloaded in November, 2014.

[23] Tartaruga, I., Cooper, J., Lowenberg, M., Sartor, P., Coggon, S., and Lemmens, Y., "Efficient Prediction and Uncertainty Propagation of Correlated Loads". *Proceedings of 56th AIAA/ASCE/AHS/ASC Structure, Structural Dynamics, and Materials Conference*, Orlando, Florida USA, January 5-9, 2015.

[24] Tartaruga, I., Cooper, J. E., Lowenberg, M. H., Sartor, P., Coggon, S., and Lemmens, Y., "Prediction and Uncertainty Propagation of Correlated Time-Varying Quantities using Surrogate Models". *CEAS*

Aeronautical Journal, DOI: 10.1007/s13272-015-0172-1.

[25] Tartaruga, I., Cooper, J. E., Lowenberg, M. H., Sartor, P., and Lemmens, Y., "Geometrical Based Method for the Uncertainty Quantification of Correlated Aircraft Loads". *ASDJournal*, 4(1), 1-20 May 2016. DOI: http://dx.doi.org/10.3293/asdj.2016.40

[26] Howcroft, C., Krauskopf, B., Lowenberg, M. H., and Neild, S. A., "Influence of Variable Side-Stay Geometry on the Shimmy Dynamics of an Aircraft Dual-Wheel Main Landing Gear", SIAM Journal on Applied Dynamical Systems, vol 12., pp. 1181-1209, 2013.

[27] Pacejka, Hans B., *Tyre and vehicle dynamics*, Second Edition, 2006 Elsevier Ltd.

[28] ICAO Doc 8168 PANS-OPS Vol 1, http://www.ce560xl.com/files downloaded in 2015.

[29] Saltelli, A., Chan, K., and Scott, E. M., *Sensitivity Analysis*. Wiley, First edition, 2009.

[30] Saltelli, A., Annoni, P., Azzini, I., Campolongo, F., Ratto, M., and Tarantola, S., "Variance based sensitivity analysis of model output. Design and estimator for the total sensitivity index". *Computer Physics Communications*, Vol. 181, pp. 259-270, 2010. DOI: 10.1016/j.cpc.2009.09.018

[31] Homma, T. & Saltelli, A., "Importance measures in global sensitivity analysis of nonlinear models". *Reliability Engineering and System Safety*, Vol. 52, pp. 1-17, 1996. DOI: 10.1016/0951-8320(96)00002-6

[32] Homma, T. & Saltelli, A., *Global Sensitivity Analysis of Nonlinear Models, Importance Measures and Sobol' Sensitivity indices*. Report EUR 16052 EN, JOINT RESEARCH CENTRE EUROPEAN COMMISSION, Environment Institute, 1994.

[33] Couckuyt, I., Dhaene, T., and Demeester, P., *ooDACE toolbox, A Matlab Kriging toolbox: Getting started*. Third edition, June, 2013. downloaded on http://www.sumo.intec.ugent.be/sites/sumo/files/gettingstarted.pdf in 2014.

[34] Joseph, R., Hung, Y., and Sudjianto, A., "Blind Kriging: A New method for Developing Surrogate models". *Journal of Mechanical Design*, Vol. 130, issue 3, 2008. DOI: 10.1115/1.2829873

[35] Couckuyt, I., Forrester, A., Gorissen, D., De Turck, F., and Dhaene, T., "Blind Kriging: Implementation and performance analysis". *Advances in Engineering Software*, Vol. 49, pp.1-113, 2012. DOI: http://dx.doi.org/10.1016/j.advengsoft.2012.03.002

[36] Sobol', I. M., "Global sensitivity indices for nonlinear mathematical models and their Monte Carlo estimates". *Mathematics and Computers in Simulation*, Vol. 55, pp. 271-280, 2001. DOI: 10.1016/S0378-4754(00)00270-6

[37] Saltelli, A., Ratto, M., Andres, T., Campolongo, F., Cariboni, J., Gatelli, D., Saisana, M., and Tarantola, S., *Global Sensitivity Analysis, The Primer*. Wiley, 2008.

[38] Nossent, J., and Bauwens, W., "Optimising the convergence of a SobolâĂŹ sensitivity analysis for an environmental model: application of an appropriate estimate for the square of the expectation value and the total variance". International Congress on Environmental Modelling and Software Managing Resources of a Limited Planet, Sixth Biennial Meeting, Leipzig, Germany R. Seppelt, A.A. Voinov, S. Lange, D. Bankamp (Eds.), 2012.

[39] Iuliano, E., and Quagliarella, D., "Evolutionary Optimization of Benchmark Aerodynamic Cases using Physics-based Surrogate Models". *Proceedings of 53rd AIAA Aerospace Science Meeting*, Kissimmee, Florida USA, January 5-9, 2015.

[40] Thota, P., Krauskopf, B., and Lowenberg, M., "Nonlinear analysis of the influene of tire inflation pressure on nose landing gear shimmy", *Journal of Aircraft*, Vol. 47, n. 5, pp. 1697-1706, 2010. DOI: http://dx.doi.org/10.2514/6.2009-6230